

LYMPHOID NEOPLASIA

Integrated mate-pair and RNA sequencing identifies novel, targetable gene fusions in peripheral T-cell lymphoma

Rebecca L. Boddicker,¹ Gina L. Razidlo,^{2,3} Surendra Dasari,⁴ Yu Zeng,^{1,5} Guangzhen Hu,¹ Ryan A. Knudson,⁶ Patricia T. Greipp,^{1,6} Jaime I. Davila,⁴ Sarah H. Johnson,^{7,8} Julie C. Porcher,¹ James B. Smadbeck,¹ Bruce W. Eckloff,⁶ Daniel D. Billadeau,³ Paul J. Kurtin,¹ Mark A. McNiven,^{2,3} Brian K. Link,⁹ Stephen M. Ansell,¹⁰ James R. Cerhan,¹¹ Yan W. Asmann,¹² George Vasmatazis,^{7,8} and Andrew L. Feldman¹

¹Department of Laboratory Medicine and Pathology, ²Center for Basic Research in Digestive Diseases, Division of Gastroenterology & Hepatology, ³Department of Biochemistry and Molecular Biology, and ⁴Division of Biomedical Statistics and Informatics, Mayo Clinic, Rochester, MN; ⁵Department of Pathology, Tongji Hospital, Tongji University School of Medicine, Shanghai, China; ⁶Medical Genome Facility, ⁷Center for Individualized Medicine, and ⁸Department of Molecular Medicine, Mayo Clinic, Rochester, MN; ⁹Department of Internal Medicine, University of Iowa Hospitals and Clinics, Iowa City, IA; ¹⁰Division of Hematology and ¹¹Department of Health Sciences Research, Mayo Clinic, Rochester, MN; and ¹²Department of Health Sciences Research, Mayo Clinic, Jacksonville, FL

Key Points

- *VAV1* rearrangements are recurrent in PTCLs, drive tumor cell growth, and can be targeted by clinically available RAC1 inhibitors.
- Integrated mate-pair/RNA sequencing of PTCLs identifies expressed fusion transcripts that represent candidate therapeutic targets.

Peripheral T-cell lymphomas (PTCLs) represent a heterogeneous group of T-cell malignancies that generally demonstrate aggressive clinical behavior, often are refractory to standard therapy, and remain significantly understudied. The most common World Health Organization subtype is PTCL, not otherwise specified (NOS), essentially a “wastebasket” category because of inadequate understanding to assign cases to a more specific diagnostic entity. Identification of novel fusion genes has contributed significantly to improving the classification, biologic understanding, and therapeutic targeting of PTCLs. Here, we integrated mate-pair DNA and RNA next-generation sequencing to identify chromosomal rearrangements encoding expressed fusion transcripts in PTCL, NOS. Two of 11 cases had novel fusions involving *VAV1*, encoding a truncated form of the *VAV1* guanine nucleotide exchange factor important in T-cell receptor signaling. Fluorescence in situ hybridization studies identified *VAV1* rearrangements in 10 of 148 PTCLs (7%). These were observed exclusively in PTCL, NOS (11%) and anaplastic large cell lymphoma (11%). In vitro, ectopic expression of a *VAV1* fusion

promoted cell growth and migration in a RAC1-dependent manner. This growth was inhibited by azathioprine, a clinically available RAC1 inhibitor. We also identified novel kinase gene fusions, *ITK-FER* and *IKZF2-ERBB4*, as candidate therapeutic targets that show similarities to known recurrent oncogenic *ITK-SYK* fusions and *ERBB4* transcript variants in PTCLs, respectively. Additional novel and potentially clinically relevant fusions also were discovered. Together, these findings identify *VAV1* fusions as recurrent and targetable events in PTCLs and highlight the potential for clinical sequencing to guide individualized therapy approaches for this group of aggressive malignancies. (*Blood*. 2016;128(9):1234-1245)

Introduction

Peripheral T-cell lymphomas (PTCLs) represent a heterogeneous group of non-Hodgkin lymphomas (NHLs) of mature T-cell origin with poor prognosis.¹ The most common subtype of PTCL in Western countries is PTCL, not otherwise specified (NOS), which has 5-year overall and failure-free survival rates of 32% and 20%, respectively.² Although less common than B-cell NHLs, the incidence of PTCL, NOS and PTCLs in general has been increasing steadily in the United States in recent years.³ By definition, PTCL, NOS includes cases failing to meet criteria for a more specific PTCL subtype and has been referred to as a “wastebasket” category.^{4,5} Therefore, PTCL, NOS is markedly heterogeneous, and a major goal of PTCL research is to identify molecular abnormalities that improve classification and identify candidate therapeutic targets.⁶

Recurrent chromosomal rearrangements giving rise to expressed fusion transcripts play a key role in the pathogenesis and clinical management of hematologic malignancies.⁷ Among PTCLs, rearrangements of the tyrosine kinase gene, *ALK*, have diagnostic, prognostic, and therapeutic significance in ALK-positive anaplastic large cell lymphoma (ALCL).⁸⁻¹⁰ In addition, rearrangements producing fusion genes involving *TP63*, *ROS1*, and *TYK2* recently have been identified in ALCLs that are negative for ALK.¹¹⁻¹⁵ However, beyond rare *ITK-SYK* fusions,¹⁶ the contribution of gene fusions to the pathogenesis of PTCL, NOS remains poorly understood.

We previously have shown the efficacy of mate-pair DNA sequencing (MPseq) to identify chromosomal rearrangements in PTCLs

Submitted March 23, 2016; accepted May 25, 2016. Prepublished online as *Blood* First Edition paper, June 13, 2016; DOI 10.1182/blood-2016-03-707141.

The online version of this article contains a data supplement.

There is an Inside *Blood* Commentary on this article in this issue.

The publication costs of this article were defrayed in part by page charge payment. Therefore, and solely to indicate this fact, this article is hereby marked “advertisement” in accordance with 18 USC section 1734.

© 2016 by The American Society of Hematology

and other human cancers.^{12,17,18} MPseq utilizes ligation of end-labeled DNA fragments followed by refragmentation and affinity purification to generate libraries of fragments containing 2 DNA sequences originally separated by a genomic distance of several kilobases. This technique has superb sensitivity for detecting rearrangements across the entire genome at a fraction of the cost of whole-genome sequencing; however, not all chromosomal rearrangements identified by MPseq involve named genes or give rise to expressed fusion transcripts. Conversely, RNA sequencing (RNAseq) preferentially identifies expressed fusion transcripts, but false positives remain a challenge due to difficulties mapping RNA reads to the genome.¹⁹ Taking advantage of the strengths of both approaches and simultaneously providing orthogonal validation of the results, we integrated MPseq and RNAseq data to identify expressed fusion transcripts in 11 cases of PTCL, NOS. We then performed further validation, functional studies, and assessment in additional PTCL tissue samples to explore potential clinical implications of selected findings.

Materials and methods

Patients and clinical samples

Eleven cases of PTCL, NOS were analyzed by integrating data from MPseq (including 2 patients reported previously¹²) and RNAseq. These cases were selected based on availability of sufficient frozen material for sequencing studies as outlined below. Data on biopsy site and treatment status at time of biopsy are presented in supplemental Table 1, available on the *Blood* Web site. Additional PTCLs (n = 137) were evaluated by fluorescence in situ hybridization (FISH) for *VAV1* rearrangements. The study was approved by Mayo Clinic and University of Iowa Institutional Review Boards.

Sequencing and bioinformatics

MP libraries were prepared from genomic DNA extracted from frozen PTCL samples using the Mate Pair Library Prep Kit (Illumina) and sequenced on a HiSeq2000 (Illumina) as previously published.^{12,17} Reads were mapped to the human genome (GRCh38/hg38) using BIMA-V3 as published.¹⁸ Candidate events were eliminated if they had mapping scores that did not meet filtering criteria; were intrachromosomal events spanning <30 000 bp; were supported by ≤ 3 fragments; or were contained within a mask table including events occurring in noncancerous samples. RNAseq was performed on RNA extracted from frozen samples and chimeric transcripts were identified using SnowShoes-FTD as published.^{12,19}

FISH

A breakpoint FISH probe flanking the *VAV1* locus on 19p13.3 was developed by labeling bacterial artificial chromosomes with SpectrumOrange (telomeric/5': RP11-134L9, RP11-479K19, RP11-828J24, RP11-114A7) or SpectrumGreen (centromeric/3': CTD-2596O14, CTD-2564J11, RP11-876D1), and interphase FISH was performed and scored on paraffin tissue sections of PTCLs as previously described.^{12,17,20} A normal intact *VAV1* gene region is indicated by a yellow signal. Disruption of the *VAV1* gene region is indicated by separation of the yellow signal into one red (5') signal and 1 green (3') signal. Two-sided χ^2 tests were used to evaluate subtype specificity.

Cell lines, transfection, and inhibitor treatment

Jurkat cells (ATCC) were maintained in RPMI, and NIH-3T3 and HEK-293T (ATCC) were maintained in Dulbecco's modified Eagle medium, all containing 10% fetal bovine serum (Clontech) and 1% penicillin/streptomycin (Gibco). They were transfected using electroporation (Jurkat) or Lipofectamine 3000 (Life Technologies; NIH-3T3 and HEK-293T). Functional experiments were performed after 24 to 72 hours. *RAC1* (Dharmacon) or control (AllStars; Qiagen) small interfering RNAs were transfected by electroporation, and cell growth was assessed at 72 hours. Cells were treated with azathioprine (Selleck) for 72 hours.

Expression plasmids

VAV1-GSS was cloned from TCL26 cDNA into TOPO-TA (Invitrogen) using primers 5'-GGCGACAGTTACAGGCAAAGAAG-3' and 5'-TAGGAGAGG AATGACAAATACAGAGG-3', sequenced verified, and cloned into pCI (Promega) using primers 5'-CTGTATGACTGCGTGGAGAATG-3' and 5'-TAG GAGAGGAATGACAAATACAGAGG-3'. *ITK-FER* was cloned into TOPO-TA from TCL72 cDNA using primers 5'-ATGAACAACCTTATCCTCCTGG-3' and 5'-AATAATGTTACTCTGCTGGAGG-3' and then shuttled into pcDNA3.1(+) (Invitrogen) using *Bam*HI and *Eco*RV restriction enzyme digestion. Human pCL2-*VAV1* was from D.D.B.

Immunofluorescence and immunoblotting

NIH-3T3 cells were transfected and replated on acid-washed coverslips after 24 hours. At 48 hours after transfection, cells were fixed, permeabilized, and stained for actin (tetramethylrhodamine-phalloidin) and *VAV1* (Abcam ab97574 and goat anti-rabbit Alexa-Fluor-488). Cells were mounted using Vectashield with 4',6-diamidino-2-phenylindole (Vector Laboratories). Fluorescence micrographs (40 \times) were captured using iVision (BioVision) and processed using Adobe Photoshop. Circularity was calculated using ImageJ (National Institutes of Health) with a value of 1 indicating a perfect circle.

Immunoblotting was performed as previously described²¹ using antibodies for pVAV1(Y174) (Abcam; EP510Y), β -actin (Novus; AC-15), *VAV1* (Cell Signaling; #2502), and *RAC1* (Millipore; clone 23A8). Proteins were detected using IRDye 800CW and 680RD antibodies (LI-COR) on the LI-COR Odyssey CLx. Rac activity was assessed using GST-PAK1-PBD (p21-binding domain) pulldown as described previously.²²

Functional assays

Cell migration was quantified by fluorometric assay 48 hours after transfection. Jurkat cells were labeled with 2 μ M Calcein AM (Molecular Probes) for 45 minutes at 37°C in serum-free RPMI. Cells were then washed, resuspended in serum-free RPMI, and added to 5- μ m inserts (Costar) equilibrated with RPMI containing 10% serum. Cells were allowed to migrate for 3 hours at 37°C and 5% CO₂. Migrated cells then were harvested and fluorescence was measured using a CytoFluor 4000 plate reader (Applied Biosystems). Percent of cells migrated was calculated by dividing the fluorescence of the migrated cell suspension by that of the starting cell suspension.

Colony formation was performed by seeding 200 cells per well of a 6-well plate at 24 hours after transfection and incubating for 8 days. Plates were imaged and counted with AlphaImager HP (ProteinSimple). Cell growth was measured by plating at 10 000 cells per well in a 96-well plate, treating for 48 to 72 hours, and incubating with 3-(4,5-dimethylthiazol-2-yl)-5-(3-carboxymethoxyphenyl)-2-(4-sulfophenyl)-2H-tetrazolium, inner salt (MTS; Promega) for 2 to 4 hours. Absorbance was measured at 490 nm. Significance was evaluated using a Student *t* test.

Results

Integrated MPseq/RNAseq identifies novel expressed fusion transcripts in PTCL, NOS

Eleven cases of PTCL, NOS were analyzed by integrated MP/RNA-sequencing (9 men and 2 women; median age, 62 years; range, 48-75 years; Table 1). The number of genomic events identified in each case by MPseq varied from 2 to 143 (378 total events; mean/case \pm standard deviation, 34 \pm 43; Figures 1A-D). Seventy-two percent of events were intrachromosomal (range/case, 42-100%; Figure 1E). One case (TCL66) showed evidence of catastrophic chromosomal rearrangement, or chromothripsis,²³ involving chromosomes 16 and 19 (Figure 1C). Sixty-five percent of events involved 1 to 2 nongenic regions (Figure 1F). An additional 11% of events were intragenic. The remaining 24% of events (n = 90) each involved 2 named genes.

Table 1. Expressed fusion transcripts identified by integrated MPseq/RNAseq in PTCL, NOS

Case	Age (years)	Sex	Diagnosis	DNA breakpoints	Fusion transcript(s)
TCL26	70	Male	PTCL, NOS	19p13.3, 20q11.22	VAV1 ↔ GSS
TCL32	72	Male	PTCL, NOS	None	None
TCL40	50	Female	PTCL, NOS	None	None
TCL65	61	Male	PTCL, NOS	3q28, 6p22.3	ATXN1 → TP63
				1p36.23, 11q24.1	CRTAM ↔ TNFRSF9
TCL66	59	Male	PTCL, NOS	16p13.3, 19q13.33	BAX → TCEB2
				19q13.2, 19q13.33	GSK3A → ZNF541
				19q13.12, 19q13.43	LOC100128398 → THAP8
TCL72	48	Male	PTCL, NOS	5q33.1, 5q33.1	ANXA6 → RBM22
				19p13.2, 19p13.2	CARM1 → ZNF627
				1p33, 1p35.3	PPP1R8 → EFCAB14
				5q21.3, 5q33.3	ITK → FER
				1p35.2, 16q22.3	PUM1 → ZFH3
				4p16.3, 4p16.3	STX18 → ZNF718
TCL75	67	Male	PTCL, NOS	2q34, 2q34	IKZF2 → ERBB4
				2q12.3, 2q13	RANBP2 → LIMS1
TCL80	56	Male	PTCL, NOS	19p13.2, 19p13.3	VAV1 ↔ MYO1F
TCL81	64	Female	PTCL, NOS	14q32.13, 14q32.2	ATG2B → CLMN
				1p13.1, 1q23.2	COPA → CD58
				1p33, 1p34.2	SZT2 → EFCAB14
TCL84	62	Male	PTCL, NOS	None	None
TCL86	75	Male	PTCL, NOS	None	None

→, gene direction of fusion transcript; ↔, reciprocal fusion transcript also present.

Among the 90 events involving 2 genes, RNAseq identified expressed fusion transcripts in 18 (mean, 1.6 fusions/case; range, 0–6 fusions/case; Table 1); 13 (72%) were derived from intrachromosomal events, identical to the proportion among all DNA events. Three DNA events yielded reciprocal fusion transcripts. All gene pairs were unique and novel except *ATXN1*→*TP63* as previously reported.¹² Two genes, *VAV1* and *EFCAB14*, were involved in fusions in >1 case.

VAV1 rearrangements are recurrent events in PTCLs and show subtype specificity

We examined *VAV1* rearrangements in greater detail because they were recurrent and because *VAV1* encodes a guanine nucleotide exchange factor (GEF) critical in T-cell receptor (TCR) signaling.^{24,25} The 2 cases showed rearrangements with *GSS* on 20q11.22 (Figure 2A) and *MYO1F* on 19p13.2, respectively. RNAseq identified reciprocal expressed fusion transcripts in both cases. *VAV1-GSS* is shown in Figure 2B and also was revalidated by Sanger sequencing (Figure 2C). We also confirmed the presence of the resultant *VAV1-GSS* fusion protein by western blot (supplemental Figure 1). *VAV1-GSS* (*GSS* exons 2-13) and *VAV1-MYO1F* (*MYO1F* exons 26-28) showed identical *VAV1* fusion sites, resulting in loss of the *VAV1* C-terminal SH3 (CSH3) domain (Figure 2D). The reciprocal fusions, *GSS-VAV1* and *MYO1F-VAV1*, encoded only the CSH3 domain of *VAV1*.

We then investigated the frequency of *VAV1* rearrangements by interphase FISH on 148 PTCLs (Table 2; Figure 2E). FISH results were 100% concordant with MPseq/RNAseq findings for the 11 cases analyzed by both methods. *VAV1* rearrangements were present in 10 of 148 cases (7%). These rearrangements were restricted solely to PTCL, NOS (5 of 45; 11%; $P = .0153$) and ALCL (5 of 47; 11%; $P = .0175$). Because some PTCLs, NOS show similarities to ALCL and may represent a pathologic spectrum characterized by CD30 expression,²⁶ we examined CD30 expression in the cases with *VAV1* rearrangements. Although all ALCLs strongly expressed CD30, 5 of 5

cases of PTCL, NOS with *VAV1* rearrangement were negative for CD30 (Figure 2F).

VAV1-GSS promotes cell migration and growth

Because the *VAV1* CSH3 domain mediates autoinhibition of *VAV1* GEF activity,²⁷ we hypothesized that *VAV1* fusions, which lack this domain, promote *VAV1* activation. Because *VAV1* mediates cytoskeletal remodeling,²⁸ we first performed immunofluorescence for actin in adherent NIH-3T3 fibroblasts transfected with *VAV1-GSS*, wild-type (wt)*VAV1*, or an empty control vector. We observed cytoskeletal rearrangement characterized by increased circularity in *VAV1-GSS* transfected cells (0.834 ± 0.033 , where 1 indicates a perfect circle) compared with either wt*VAV1* (0.765 ± 0.048 ; $P = .045$) or control (0.453 ± 0.089 ; $P < .0001$; Figure 3A-B).

We then examined the effect of the *VAV1-GSS* fusion protein on migration and growth in the neoplastic T-cell line, Jurkat. *VAV1-GSS* was phosphorylated at *VAV1*(Y174), indicative of GEF activity²⁹ (Figure 3C). Cells expressing *VAV1-GSS* also showed increased migration (124% of empty vector control, $P = .0016$; $P = .05$ vs wt*VAV1*; Figure 3D). Finally, *VAV1-GSS* strongly promoted cell growth (159% of empty vector control; $P < .0001$ vs both control and wt*VAV1*; Figure 3E).

VAV1-GSS drives growth through RAC1 and can be targeted by Rac inhibition

Because *VAV1* GEF activity predominantly targets the Rho family GTPase RAC1 (and to a lesser extent RHOA and CDC42),^{30,31} and RAC1 has been demonstrated to promote migration in an ALCL model,³² we measured Rac activation following *VAV1-GSS* transfection in Jurkat cells. *VAV1-GSS* overexpression increased active Rac (GTP-Rac; 173% of control; $P = .054$; Figure 4A-B). Furthermore, *RAC1* knockdown abrogated the growth advantage conferred by *VAV1-GSS*, reducing growth from 125% to 102% of the baseline control value ($P = .0004$; Figure 4C). *RAC1* knockdown had no effect on growth of control-transfected Jurkat cells. These data indicate that *VAV1-GSS* function is at least in part RAC1 dependent.

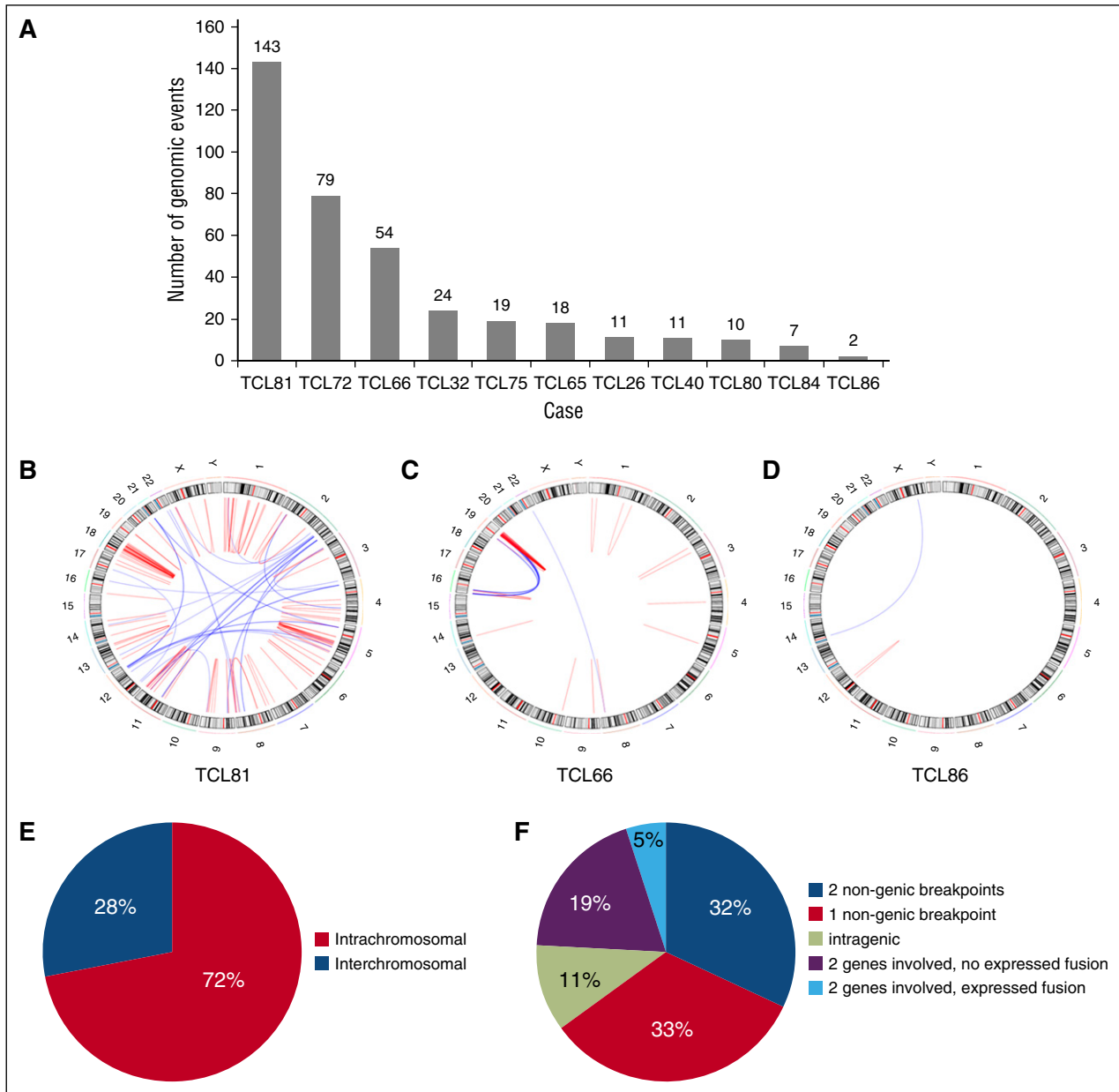


Figure 1. Distribution of 378 genomic events identified by mate-pair sequencing in 11 cases of PTCL, NOS. (A) Number of genomic events per case. (B-D) Representative Circos diagrams illustrating heterogeneity in the degree of complexity of genomic events among PTCLs: (B) high complexity; (C) focally high complexity with multiple rearrangements involving chromosomes 16 and 19 (chromothripsis); and (D) low complexity. (E) Distribution of intrachromosomal and interchromosomal events. (F) Distribution of events based on involvement of genes or nongenic regions and identification of expression fusion transcripts by RNA sequencing.

We then treated transfected Jurkat cells with azathioprine, a clinically available immunosuppressant and Rac inhibitor.³³⁻³⁵ At a dose of 10 μ M, azathioprine inhibited growth of *VAV1-GSS*-transfected cells by $79.4 \pm 1.4\%$ compared with $26.0 \pm 2.0\%$ in control-transfected cells ($P < .0001$), and $62.1 \pm 4.5\%$ in wt*VAV1*-transfected cells ($P = .0001$; Figure 4D). Taken together, these findings demonstrate that *VAV1-GSS* promotes increased GEF activity and Rac activation that drives cell migration and growth and confers enhanced sensitivity to Rac inhibition.

MPseq/RNAseq identifies novel kinase fusions in PTCL, NOS

Among the other events identified by MPseq/RNAseq (Table 1) were fusions involving kinase genes known to be involved in oncogenic

events in other cancers. Case *TCL72* had an in-frame *ITK-FER* fusion (Figure 5A-C). Although *ITK* is expressed consistently in PTCL, NOS,³⁶ read-count data showed *FER* expression only in *TCL72* exons 11 to 20 encoded by *ITK-FER* (Figure 5D). Of note, *ITK-SYK* fusions are recurrent in PTCL, NOS and *SYK* inhibitors have been proposed therapeutically.^{16,37} *ITK*, *SYK*, and *FER* all encode SH2 domain-containing nonreceptor tyrosine kinases.³⁸ Like *ITK-SYK*, *ITK-FER* retains the N-terminal plekstrin homology domain of *ITK* required for *ITK-SYK* function³⁹ and contains the *FER* C-terminal kinase domain in place of the *SYK* kinase domain (Figure 5E).¹⁶ In line with this, expression of *ITK-FER* in HEK-293T cells resulted in increased colony formation (148% of control, $P = .0001$; Figure 5F). *FER* fusions have not been reported in PTCLs, although an *SSBP2-FER* fusion has been reported in T-cell acute lymphoblastic leukemia.⁴⁰ *FER* is sensitive to

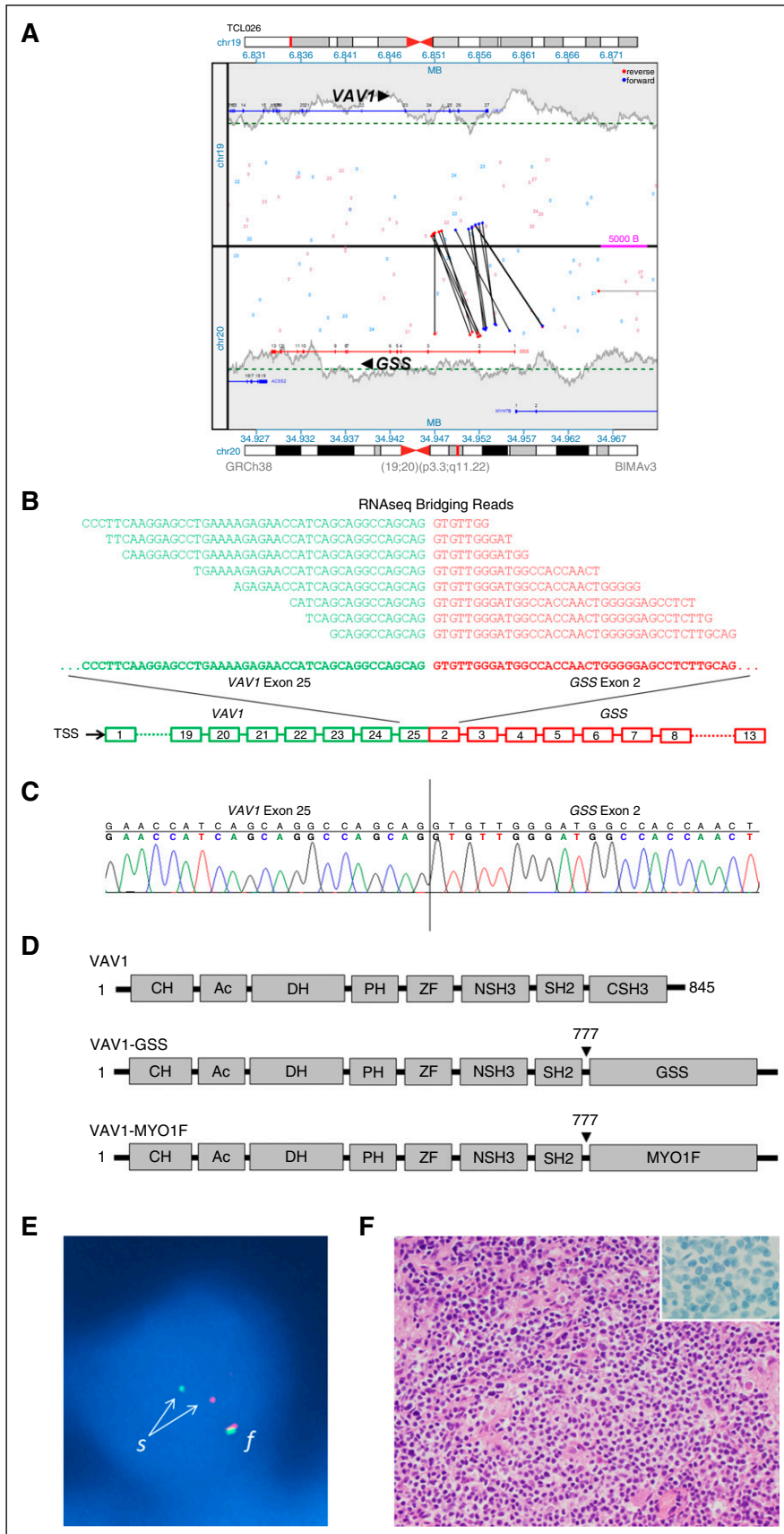


Figure 2. Identification and validation of VAV1 fusions in PTCL, NOS. (A) Rearrangement of VAV1 and GSS genes as detected in genomic DNA by MPseq. Vertical and oblique black lines represent aberrant read-pairs; blue ends indicate mapping to (+) strand, whereas red ends indicate mapping to (-) strand. (B) VAV1-GSS fusion transcript as detected by RNAseq. Bridging reads spanning the fusion site are shown. TSS, transcription start site. (C) Sanger sequencing of the fusion site in VAV1-GSS fusion. (D) Schematic diagrams of VAV1 protein domains in wild-type VAV1 and resulting from VAV1 fusions. (E) FISH confirming a VAV1 rearrangement in a tumor cell nucleus (blue) from a PTCL, NOS specimen. The normal intact VAV1 allele is indicated by a red-green fusion (f) signal. Disruption of the VAV1 gene region on the other allele is indicated by separation (s) into one red (5') signal and 1 green (3') signal. (F) Pathologic features of PTCL, NOS with VAV1 fusion (hematoxylin and eosin stain; inset, CD30 immunostain). Original magnification $\times 400$ (inset, $\times 1000$).

Table 2. Frequency of VAV1 rearrangements in 148 PTCLs

	MP/RNA cases*			Additional FISH cases			Total			P value†
	n positive	n tested	%	n positive	n tested	%	n positive	n tested	%	
PTCL, NOS	2	11	18	3	34	9	5	45	11	0.0153
AITL	0	0	—	0	36	0	0	36	0	—
ALCL	0	0	—	5	47	11	5	47	11	0.0175
ALK ⁺	0	0	—	1	18	6	1	18	6	0.2685
ALK ⁻	0	0	—	4	25	16	4	25	16	0.0060
Cutaneous	0	0	—	0	4	0	0	4	0	—
EATL	0	0	—	0	5	0	0	5	0	—
NKTL	0	0	—	0	7	0	0	7	0	—
CTCL	0	0	—	0	6	0	0	6	0	—
T-LGL	0	0	—	0	2	0	0	2	0	—
Total	2	11	18	8	137	6	10	148	7	—

Bold entries denote statistical significance, $P < .05$.

AITL, angioimmunoblastic T-cell lymphoma; ALK, anaplastic lymphoma kinase; CTCL, cutaneous T-cell lymphoma; EATL, enteropathy-associated T-cell lymphoma; NKTL, extranodal NK-/T-cell lymphoma, nasal type; T-LGL, T-cell large granular lymphocytic leukemia.

*All cases also tested by FISH with 100% concordance.

†Versus AITL, EATL, NKTL, CTCL, and T-LGL together.

kinase inhibitors under evaluation, including aminopyridine 8e, a drug developed to target mutant ALK.⁴¹

We also identified a novel *IKZF2-ERBB4* fusion in case TCL75 (supplemental Figure 2A-C). *IKZF2* encodes Helios, a T cell–restricted Ikaros-family transcription factor, and is expressed in various PTCLs.⁴²⁻⁴⁵ *IKZF2* was expressed similarly in TCL75 and other cases, whereas *ERBB4* was expressed only in TCL75 exons 2 to 28 encoded by *IKZF2-ERBB4*, which includes the ERBB4 kinase domain (supplemental Figure D-E). Thus, the fusion, which contains only exons 1 to 2 of *IKZF2*, co-opts the *IKZF2* promoter for expression.⁴⁶ These findings complement a recent report of truncated *ERBB4* transcripts promoted by intronic long terminal repeats in ALCL, which retain ERBB4 kinase activity and are sensitive to ERBB family kinase inhibitors such as lapatinib.⁴⁷

Examination of exon-level read plots for genes involved in the remaining fusions in Table 1 demonstrated 2 additional events with altered read counts in the case of interest: diminished *CD58* expression in TCL81 (*COPA-CD58* fusion; supplemental Figure 3A) and increased *ZNF541* expression (exons 11-15) in TCL66 (*GSK3A-ZNF541* fusion; supplemental Figure 3B).

Discussion

Here, we integrated MPseq and RNAseq data to identify expressed fusion transcripts in PTCL, NOS, an aggressive malignancy that is the most common form of T-cell NHL.² Our findings highlight the marked genomic heterogeneity underlying this disorder, both in overall structural complexity and in the distribution of specific genetic events. We identified recurrent, novel, and targetable rearrangements of the *VAV1* gene, which encodes a critical component of TCR signaling. We also discovered novel kinase fusions that represent candidate therapeutic targets. These data suggest that clinical sequencing approaches may help match PTCL patients to targeted therapeutics for personalized cancer therapy.

We identified *VAV1* rearrangements in 11% of PTCL, NOS and ALCL, but not in other PTCL subtypes, suggesting that the biologic role of the resultant fusion proteins in T-cell lymphomagenesis may be highly context dependent. Of note, knockdown of *VAV1* previously has been shown to lead to cell cycle arrest and apoptosis of ALCL cells.⁴⁸ In addition, predicted gain-of-function hotspot mutations of *VAV1*

recently have been reported in adult T-cell leukemia/lymphoma (ATL).⁴⁹ ATL was not evaluated in our study group as it is associated with human T-cell leukemia virus type-1 infection, which is non-endemic in the Midwestern United States.

We demonstrated that *VAV1* fusions increased Rac activation and promoted cell growth. We focused on RAC1 because mutation of the VAV1 CSH3 domain strongly activates RAC1, whereas its effects on the ρ GTPases CDC42 and RHOA are more modest.²⁷ RAC1 also has been shown to be activated by NPM-ALK in ALCL cells, and a Rac small molecule inhibitor blocked lymphoma development and dissemination.^{50,51} We showed that cells expressing VAV1-GSS were exquisitely sensitive to azathioprine, which inhibits activation of RAC1 but not of CDC42 or RHOA.^{33,34} Other clinically available drugs that inhibit RAC1 and have been proposed to be repurposed as anticancer agents include metformin, statins such as simvastatin, and R-ketorolac.⁵²⁻⁵⁴ RAC1 small molecule inhibitors are in ongoing development.^{55,56} Taken together, these data suggest RAC1 inhibition is a potential therapeutic strategy for PTCLs with *VAV1* fusions, noting, however, that these fusions are present in the minority of PTCLs.

Our data add to a growing body of evidence supporting the importance of ρ -family GTPases in PTCL, including recently reported *RHOA* mutations in PTCL, NOS and angioimmunoblastic T-cell lymphomas⁵⁷⁻⁵⁹ and redundant and nonredundant roles for RAC1 and CDC42 in ALCL cell growth, migration, and dissemination.^{32,48} More broadly, these findings suggest the importance of TCR signaling as a key pathway involved in lymphomagenesis,⁶⁰ as has been demonstrated in mice⁶¹ and is evidenced further by other genes altered by various mechanisms in PTCLs, including rearrangements of *SYK*, copy number gains of *ITK*, and point mutations of *FYN*.^{16,49,57,62} These potentially targetable molecular alterations show promise for advances analogous to those resulting from elucidation of dysregulated B-cell receptor signaling in B-cell NHLs.^{63,64}

It should be noted that, in addition to the RAC1-mediated effects we demonstrated in *VAV1-GSS*-transfected cells, VAV1 has non-GEF-associated functions in T cells as well.⁶⁵ For example, loss of the VAV1 CSH3 domain also might increase activity of nuclear factor of activated T cells through loss of nuclear factor of activated T cells–inhibitory residues.⁶⁶ RAC1 also has multiple mechanisms of oncogenic activity, including its ability to enhance cytokine-mediated activation of signal transducer and activator of transcription 3 (STAT3),⁶⁷ which plays a central pathogenetic role in many PTCLs.^{14,68-71} Finally, the role of the

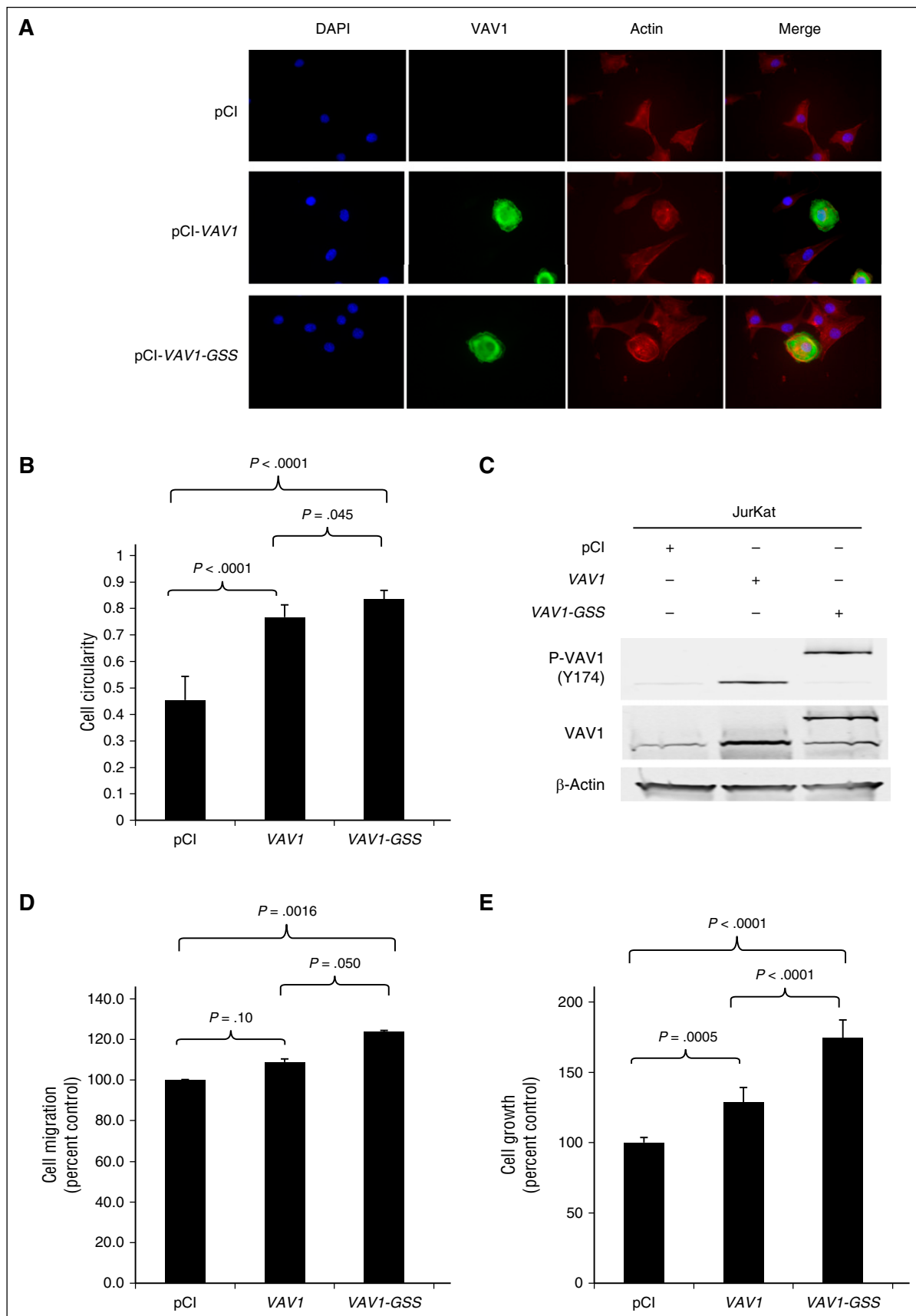


Figure 3. VAV1-GSS fusion drives cytoskeletal reorganization, migration, and proliferation. (A) VAV1-GSS fusion promotes cytoskeletal reorganization and (B) increased cell circularity in adherent NIH-3T3 cells. A circularity value of 1 indicates a perfect circle. (C) The VAV1-GSS fusion protein is phosphorylated at VAV1 Y174 in Jurkat cells. In Jurkat, VAV1-GSS drives cell (D) migration and (E) growth relative to both wild-type VAV1 and an empty vector control.

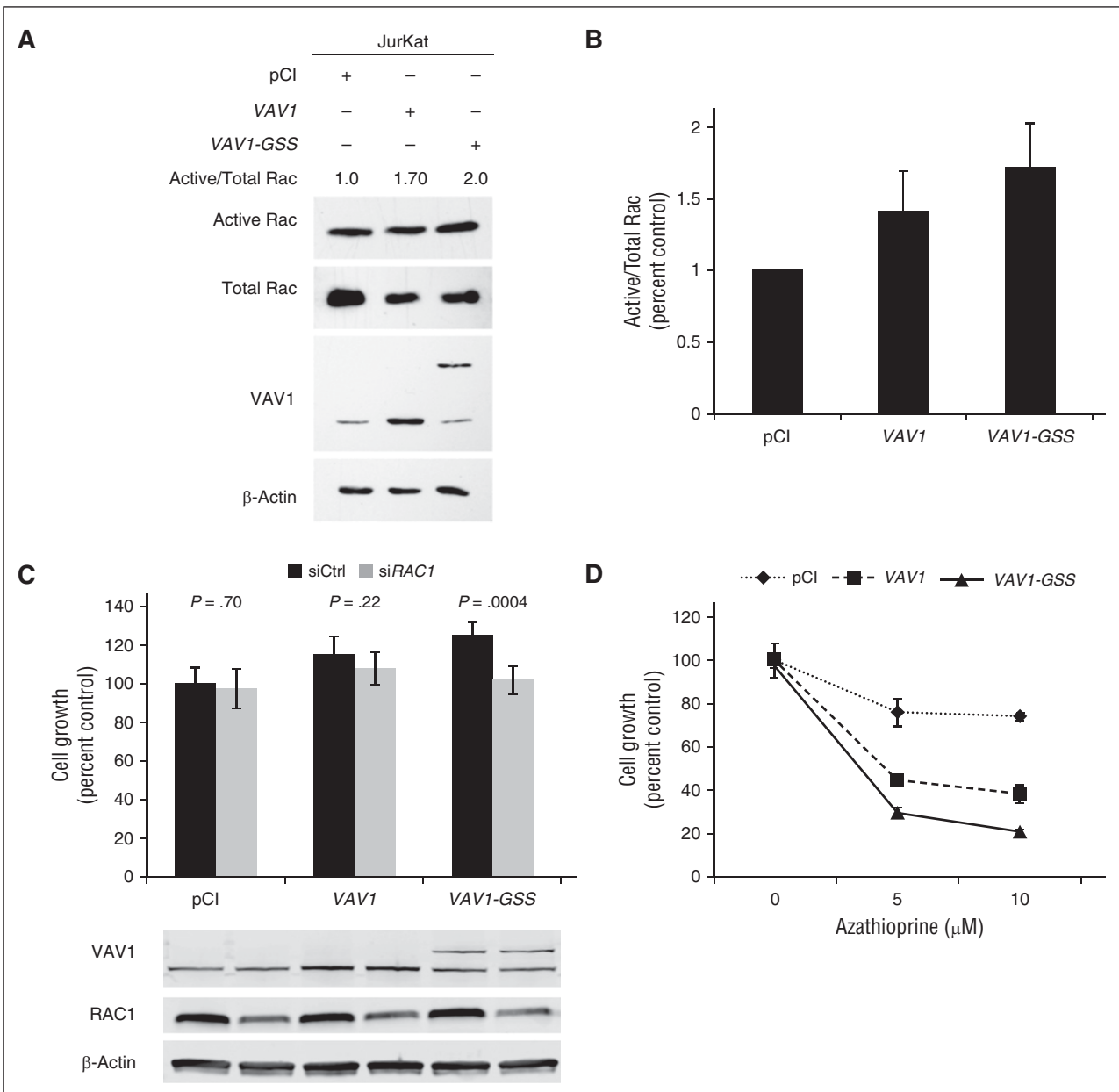


Figure 4. VAV1-GSS fusion induces targetable RAC1 dependence. (A) VAV1-GSS fusion induces Rac activation in Jurkat cells. (B) Rac activation data summarizing 3 independent experiments as shown in A. (C) RAC1 knock-down abrogates effect of VAV1-GSS fusion on cell growth. (D) Jurkat cells transfected with VAV1-GSS exhibit greater sensitivity to azathioprine than cells transfected with wild-type VAV1 or an empty vector control.

partner gene in VAV1 fusions, as well the potential function of the reciprocal expressed transcripts, may merit further study.

Our institution and others have developed clinical infrastructure to facilitate a personalized medicine approach to malignant diseases, in which genomic testing might inform therapeutic strategies specific for each individual.⁷² Although this concept is still evolving, data on PTCLs from our group and others, as well as our institutional experience with an Individualized Medicine Clinic, suggest PTCL patients might be particularly suitable for this approach.^{13,73-75} PTCLs are relatively uncommon and generally are clinically aggressive. They are markedly heterogeneous, both at the genetic-biologic level and at the clinicopathologic level, with >15 subtypes recognized by the World Health Organization.⁷⁶ Current standard therapy is acknowledged to be sub-optimal, but a number of targeted agents have shown clinical efficacy in

subsets of patients.^{1,74} With this in mind, we examined the events identified by MPseq/RNAseq for their potential to suggest therapeutic options.

In addition to VAV1 rearrangements, we also discovered 2 novel kinase gene fusions, *ITK-FER* and *IKZF2-ERBB4*. As previously exemplified among PTCLs by *ALK* fusions, both fusions resulted in overexpression of a kinase not normally expressed in the cell-of-origin under the control of the partner gene promoter. In keeping with its predicted oncogenic function, *ITK-FER* promoted colony formation in vitro. *ERBB4* encodes a member of the ERBB family, a group of targetable receptor tyrosine kinases that also includes epidermal growth factor receptor (ERBB1), HER2 (ERBB2), and ERBB3, and historically has been associated with the pathogenesis of epithelial and other solid tumors.⁷⁷ Recent data, however, support the relevance of this family in PTCLs, including aberrant *ERBB4* transcripts, elevated

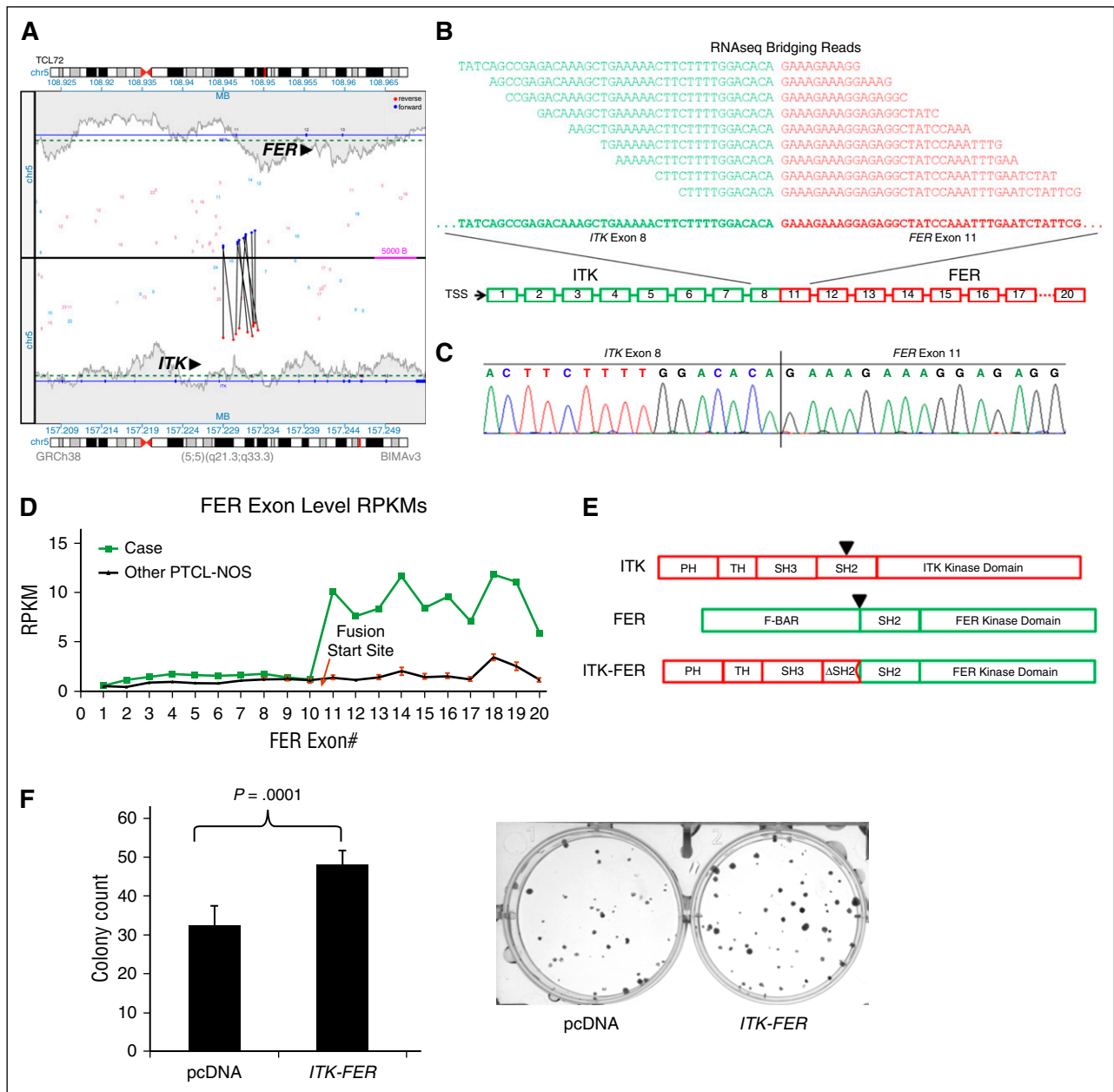


Figure 5. Novel *ITK-FER* kinase fusion in PTCL, NOS. (A) *ITK-FER* rearrangement as detected by MPseq. (B) *ITK-FER* fusion transcript as detected by RNAseq. (C) Sanger sequencing of the *ITK-FER* fusion site. (D) Exon-level RNAseq read plot for *FER* in TCL72 ("Case") compared with the remaining 10 sequenced cases of PTCL, NOS. RPKM, reads per kilobase per million. (E) Schematic diagrams of protein domains in ITK, FER, and the ITK-FER fusion protein. (F) *ITK-FER* expression promotes colony formation in HEK-293 cells. PH, pleckstrin homology; TH, Tec homology; SH, Src homology; F-BAR, FER-CIP4 homology–Bin-amphiphysin-Rvs.

circulating epidermal growth factor levels, and enrichment for somatic mutations targeting the ERBB signaling pathway.^{47,78,79}

We also rediscovered a previously reported *ATXN1-TP63* fusion. *TP63* rearrangements are recurrent in PTCL, NOS and ALK-negative ALCL and are characterized by high proliferation indices and poor prognosis.^{12,13} In fact, this patient (TCL65) had aggressive disease refractory to multiple regimens, did not achieve a response sufficient to be transplant eligible, and died 13 months after diagnosis. Poor outcomes with standard therapy suggest that patients with *TP63*-rearranged PTCLs might be considered for more intensive or experimental upfront treatment approaches.^{12,13}

We identified 2 other genes, *CD58* and *ZNF541*, whose expression differed between rearranged and nonrearranged cases. TCL81 carried a

COPA-CD58 rearrangement associated with decreased *CD58* expression. *CD58* encodes a member of the immunoglobulin superfamily, *CD58/LFA-3*, an adhesion molecule known to be genetically inactivated by deletions and mutations in B-cell NHLs as a mechanism of immune escape.⁸⁰ Deletions and mutations, but not rearrangements, of *CD58* recently have been reported in PTCLs as well.^{57,58,81} Rearrangements are a less common structural cause of gene inactivation than deletions but have been reported. For example, we have shown that rearrangements disrupting the *DUSP22* phosphatase gene are associated with decreased expression of the putative tumor suppressor gene, *DUSP22*, in ALCL.¹⁷ We also identified marked expression of *ZNF541* only in TCL66, which carried a *GSK3A-ZNF541* fusion. *GSK3A*, which was ubiquitously expressed in all sequenced samples (data not shown), encodes glycogen

synthase kinase-3a, which itself has been proposed as a therapeutic target in cancer.⁸² ZNF541 normally is expressed in germ cells, where it mediates chromatin remodeling and is associated with histone hypoacetylation.⁸³ Notably, treatment with histone deacetylase inhibitors, a class of drugs US Food and Drug Administration approved for PTCL,⁷⁴ dramatically reduced ZNF541 protein levels.

EFCAB14 was involved in fusions in 2 of 11 sequenced cases. This gene encodes a member of the EF-hand superfamily of calcium-binding proteins, which play a role in TCR signaling.⁸⁴ In 1 of these cases (TCL72), *EFCAB14* was fused to *PPP1R8*, which encodes a phosphatase inhibitor critical for the activity of EZH2, a promising therapeutic target in PTCL.^{85,86} We also identified a reciprocal fusion of *TNFRSF9* (TCL65) encoding CD137/4-1BB, a costimulatory molecule proposed as a therapeutic target in PTCL.⁸⁷ Of note, fusions and mutations affecting the costimulatory molecules CD28 and ICOS recently have been observed in PTCL.^{49,88} We also identified a fusion involving the proapoptotic gene, *BAX* (TCL66), which has been reported to undergo loss-of-function mutations, but not rearrangements, in hematologic malignancies.⁸⁹ Sequencing of additional PTCLs is likely to help prioritize these events for further study and identify additional candidates.

Acknowledgments

This work was supported by awards R01 CA177734 (A.L.F.), P30 CA15083 (Mayo Clinic Cancer Center), and P50 CA97274 (University of Iowa/Mayo Clinic Lymphoma Specialized Program of Research

Excellence) from the National Institutes of Health, National Cancer Institute, the Fraternal Order of Eagles Cancer Research Fund, Mayo Clinic Cancer Center (R.L.B. and G.L.R.), Clinical and Translational Science Award grant UL1 TR000135 from the National Center for Advancing Translational Science, award CI-48-09 from the Damon Runyon Cancer Research Foundation (A.L.F.), a scholarship award from the China Scholarship Council (Y.Z.), the Center for Individualized Medicine and the Department of Laboratory Medicine and Pathology, Mayo Clinic; and the Predolin Foundation.

Authorship

Contribution: R.L.B. and A.L.F. designed the study and wrote the manuscript; D.D.B., M.A.M., and G.V. contributed to study design; R.L.B., G.L.R., Y.Z., G.H., J.C.P., and B.W.E. conducted experiments; R.L.B., S.D., J.I.D., S.H.J., J.B.S., Y.W.A., G.V., and A.L.F. analyzed data; R.A.K. and P.T.G. conducted cytogenetic studies; and P.J.K., B.K.L., S.M.A., and J.R.C. contributed clinical specimens.

Conflict-of-interest disclosure: The authors declare no competing financial interests.

Correspondence: Andrew L. Feldman, Department of Laboratory Medicine and Pathology, Mayo Clinic, 200 First Street SW, Rochester, MN 55905; e-mail: feldman.andrew@mayo.edu; or George Vasmatazis, Center for Individualized Medicine, Mayo Clinic, 200 First St SW, Rochester, MN 55905; e-mail: vasmatazis.george@mayo.edu.

References

- Armitage JO. The aggressive peripheral T-cell lymphomas: 2012 update on diagnosis, risk stratification, and management. *Am J Hematol*. 2012;87(5):511-519.
- Vose J, Armitage J, Weisenburger D; International T-Cell Lymphoma Project. International peripheral T-cell and natural killer/T-cell lymphoma study: pathology findings and clinical outcomes. *J Clin Oncol*. 2008;26(25):4124-4130.
- Abouyabis AN, Shenoy PJ, Lechowicz MJ, Flowers CR. Incidence and outcomes of the peripheral T-cell lymphoma subtypes in the United States. *Leuk Lymphoma*. 2008;49(11):2099-2107.
- Pileri SA, et al. Peripheral T-cell lymphoma, not otherwise specified. In: Swerdlow S, et al, eds. WHO Classification of Tumours of Haematopoietic and Lymphoid Tissues. Lyon: International Agency for Research on Cancer; 2008:306-308.
- Jaffe ES. The 2008 WHO classification of lymphomas: implications for clinical practice and translational research. *Hematology Am Soc Hematol Educ Program*. 2009;2009:523-531.
- Attygalle AD, Cabeçadas J, Gaulard P, et al. Peripheral T-cell and NK-cell lymphomas and their mimics; taking a step forward - report on the lymphoma workshop of the XVIth meeting of the European Association for Haematopathology and the Society for Hematopathology. *Histopathology*. 2014;64(2):171-199.
- Rowley JD. Chromosomal translocations: revisited yet again. *Blood*. 2008;112(6):2183-2189.
- Jaffe ES. Anaplastic large cell lymphoma: the shifting sands of diagnostic hematopathology. *Mod Pathol*. 2001;14(3):219-228.
- Foyil KV, Bartlett NL. Brentuximab vedotin and crizotinib in anaplastic large-cell lymphoma. *Cancer J*. 2012;18(5):450-456.
- Gascoyne RD, Aoun P, Wu D, et al. Prognostic significance of anaplastic lymphoma kinase (ALK) protein expression in adults with anaplastic large cell lymphoma. *Blood*. 1999;93(11):3913-3921.
- Morris SW, Kirstein MN, Valentine MB, et al. Fusion of a kinase gene, ALK, to a nucleolar protein gene, NPM, in non-Hodgkin's lymphoma. *Science*. 1994;263(5151):1281-1284.
- Vasmatazis G, Johnson SH, Knudson RA, et al. Genome-wide analysis reveals recurrent structural abnormalities of TP63 and other p53-related genes in peripheral T-cell lymphomas. *Blood*. 2012;120(11):2280-2289.
- Parrilla Castellar ER, Jaffe ES, Said JW, et al. ALK-negative anaplastic large cell lymphoma is a genetically heterogeneous disease with widely disparate clinical outcomes. *Blood*. 2014;124(9):1473-1480.
- Crescenzo R, Abate F, Lasorsa E, et al. Convergent mutations and kinase fusions lead to oncogenic STAT3 activation in anaplastic large cell lymphoma. *Cancer Cell*. 2015;27(4):516-532.
- Velusamy T, Kiel MJ, Sahasrabudhe AA, et al. A novel recurrent NPM1-TYK2 gene fusion in cutaneous CD30-positive lymphoproliferative disorders. *Blood*. 2014;124(25):3768-3771.
- Streubel B, Vinatzer U, Willheim M, Raderer M, Chott A. Novel t(5;9)(q33;q22) fuses ITK to SYK in unspecified peripheral T-cell lymphoma. *Leukemia*. 2006;20(2):313-318.
- Feldman AL, Dogan A, Smith DI, et al. Discovery of recurrent t(6;7)(p25.3;q32.3) translocations in ALK-negative anaplastic large cell lymphomas by massively parallel genomic sequencing. *Blood*. 2011;117(3):915-919.
- Drucker TM, Johnson SH, Murphy SJ, Cradic KW, Therneau TM, Vasmatazis G. BIMA V3: an aligner customized for mate pair library sequencing. *Bioinformatics*. 2014;30(11):1627-1629.
- Asmann YW, Hossain A, Necela BM, et al. A novel bioinformatics pipeline for identification and characterization of fusion transcripts in breast cancer and normal cell lines. *Nucleic Acids Res*. 2011;39(15):e100.
- Feldman AL, Law M, Grogg KL, et al. Incidence of TCR and TCL1 gene translocations and isochromosome 7q in peripheral T-cell lymphomas using fluorescence in situ hybridization. *Am J Clin Pathol*. 2008;130(2):178-185.
- Boddicker RL, Kip NS, Xing X, et al. The oncogenic transcription factor IRF4 is regulated by a novel CD30/NF-κB positive feedback loop in peripheral T-cell lymphoma. *Blood*. 2015;125(20):3118-3127.
- Razidlo GL, Wang Y, Chen J, Krueger EW, Billadeau DD, McNiven MA. Dynamin 2 potentiates invasive migration of pancreatic tumor cells through stabilization of the Rac1 GEF Vav1. *Dev Cell*. 2013;24(6):573-585.
- Stephens PJ, Greenman CD, Fu B, et al. Massive genomic rearrangement acquired in a single catastrophic event during cancer development. *Cell*. 2011;144(1):27-40.
- Fischer KD, Zmudzinas A, Gardner S, Barbacid M, Bernstein A, Guidos C. Defective T-cell receptor signalling and positive selection of Vav-deficient CD4+ CD8+ thymocytes. *Nature*. 1995;374(6521):474-477.
- Tybulewicz VL. Vav-family proteins in T-cell signalling. *Curr Opin Immunol*. 2005;17(3):267-274.

26. Xing X, Feldman AL. Anaplastic large cell lymphomas: ALK positive, ALK negative, and primary cutaneous. *Adv Anat Pathol*. 2015;22(1):29-49.
27. Barreira M, Fabbiano S, Couceiro JR, et al. The C-terminal SH3 domain contributes to the intramolecular inhibition of Vav family proteins. *Sci Signal*. 2014;7(321):ra35.
28. Villalba M, Bi K, Rodriguez F, Tanaka Y, Schoenberger S, Altman A. Vav1/Rac-dependent actin cytoskeleton reorganization is required for lipid raft clustering in T cells. *J Cell Biol*. 2001;155(3):331-338.
29. Miletic AV, Sakata-Sogawa K, Hiroshima M, et al. Vav1 acidic region tyrosine 174 is required for the formation of T cell receptor-induced microclusters and is essential in T cell development and activation. *J Biol Chem*. 2006;281(50):38257-38265.
30. Crespo P, Schuebel KE, Ostrom AA, Gutkind JS, Bustelo XR. Phosphotyrosine-dependent activation of Rac-1 GDP/GTP exchange by the vav proto-oncogene product. *Nature*. 1997;385(6612):169-172.
31. Turner M, Billadeau DD. VAV proteins as signal integrators for multi-subunit immune-recognition receptors. *Nat Rev Immunol*. 2002;2(7):476-486.
32. Choudhari R, Minero VG, Menotti M, et al. Redundant and nonredundant roles for Cdc42 and Rac1 in lymphomas developed in NPM-ALK transgenic mice. *Blood*. 2016;127(10):1297-1306.
33. Poppe D, Tiede I, Fritz G, et al. Azathioprine suppresses ezrin-radixin-moesin-dependent T cell-APC conjugation through inhibition of Vav guanosine exchange activity on Rac proteins. *J Immunol*. 2006;176(1):640-651.
34. Tiede I, Fritz G, Strand S, et al. CD28-dependent Rac1 activation is the molecular target of azathioprine in primary human CD4+ T lymphocytes. *J Clin Invest*. 2003;111(8):1133-1145.
35. Razidlo GL, Magnine C, Sletten AC, et al. Targeting Pancreatic Cancer Metastasis by Inhibition of Vav1, a Driver of Tumor Cell Invasion. *Cancer Res*. 2015;75(14):2907-2915.
36. Agostinelli C, Rizvi H, Paterson J, et al. Intracellular TCR-signaling pathway: novel markers for lymphoma diagnosis and potential therapeutic targets. *Am J Surg Pathol*. 2014;38(10):1349-1359.
37. Wilcox RA, Sun DX, Novak A, Dogan A, Ansell SM, Feldman AL. Inhibition of Syk protein tyrosine kinase induces apoptosis and blocks proliferation in T-cell non-Hodgkin's lymphoma cell lines. *Leukemia*. 2010;24(1):229-232.
38. Gocek E, Moulas AN, Studzinski GP. Non-receptor protein tyrosine kinases signaling pathways in normal and cancer cells. *Crit Rev Clin Lab Sci*. 2014;51(3):125-137.
39. Rigby S, Huang Y, Streubel B, et al. The lymphoma-associated fusion tyrosine kinase ITK-SYK requires pleckstrin homology domain-mediated membrane localization for activation and cellular transformation. *J Biol Chem*. 2009;284(39):26871-26881.
40. Atak ZK, Gianfelici V, Hulselms G, et al. Comprehensive analysis of transcriptome variation uncovers known and novel driver events in T-cell acute lymphoblastic leukemia. *PLoS Genet*. 2013;9(12):e1003997.
41. Huang Q, Johnson TW, Bailey S, et al. Design of potent and selective inhibitors to overcome clinical anaplastic lymphoma kinase mutations resistant to crizotinib. *J Med Chem*. 2014;57(4):1170-1187.
42. Hahm K, Cobb BS, McCarty AS, et al. Helios, a T cell-restricted Ikaros family member that quantitatively associates with Ikaros at centromeric heterochromatin. *Genes Dev*. 1998;12(6):782-796.
43. Iqbal J, Weisenburger DD, Chowdhury A, et al; International Peripheral T-cell Lymphoma Project. Natural killer cell lymphoma shares strikingly similar molecular features with a group of non-hepatosplenic $\gamma\delta$ T-cell lymphoma and is highly sensitive to a novel aurora kinase A inhibitor in vitro. *Leukemia*. 2011;25(2):348-358.
44. Fujiwara SI, Yamashita Y, Nakamura N, et al. High-resolution analysis of chromosome copy number alterations in angioimmunoblastic T-cell lymphoma and peripheral T-cell lymphoma, unspecified, with single nucleotide polymorphism-typing microarrays. *Leukemia*. 2008;22(10):1891-1898.
45. Fujii K, Ishimaru F, Nakase K, et al. Over-expression of short isoforms of Helios in patients with adult T-cell leukaemia/lymphoma. *Br J Haematol*. 2003;120(6):986-989.
46. Fujimoto R, Ozawa T, Itoyama T, Sadamori N, Kurosawa N, Isobe M. HELIOS-BCL11B fusion gene involvement in a t(2;14)(q34;q32) in an adult T-cell leukemia patient. *Cancer Genet*. 2012;205(7-8):356-364.
47. Scartò I, Pellegrino E, Mereu E, et al; European T-Cell Lymphoma Study Group. Identification of a new subclass of ALK-negative ALCL expressing aberrant levels of ERBB4 transcripts. *Blood*. 2016;127(2):221-232.
48. Ambrogio C, Voena C, Manazza AD, et al. The anaplastic lymphoma kinase controls cell shape and growth of anaplastic large cell lymphoma through Cdc42 activation. *Cancer Res*. 2008;68(21):8899-8907.
49. Kataoka K, Nagata Y, Kitanaka A, et al. Integrated molecular analysis of adult T cell leukemia/lymphoma. *Nat Genet*. 2015;47(11):1304-1315.
50. Colomba A, Courilleau D, Ramel D, et al. Activation of Rac1 and the exchange factor Vav3 are involved in NPM-ALK signaling in anaplastic large cell lymphomas. *Oncogene*. 2008;27(19):2728-2736.
51. Colomba A, Giurinto S, Dejean E, et al. Inhibition of Rac controls NPM-ALK-dependent lymphoma development and dissemination. *Blood Cancer J*. 2011;1(6):e21.
52. Dirat B, Ader I, Golzio M, et al. Inhibition of the GTPase Rac1 mediates the antimigratory effects of metformin in prostate cancer cells. *Mol Cancer Ther*. 2015;14(2):586-596.
53. Guo Y, Kenney SR, Muller CY, et al. R-Ketorolac Targets Cdc42 and Rac1 and Alters Ovarian Cancer Cell Behaviors Critical for Invasion and Metastasis. *Mol Cancer Ther*. 2015;14(10):2215-2227.
54. Miller T, Yang F, Wise CE, et al. Simvastatin stimulates apoptosis in cholangiocarcinoma by inhibition of Rac1 activity. *Dig Liver Dis*. 2011;43(5):395-403.
55. Nassar N, Cancelas J, Zheng J, Williams DA, Zheng Y. Structure-function based design of small molecule inhibitors targeting Rho family GTPases. *Curr Top Med Chem*. 2006;6(11):1109-1116.
56. Lin Y, Zheng Y. Approaches of targeting Rho GTPases in cancer drug discovery. *Expert Opin Drug Discov*. 2015;10(9):991-1010.
57. Palomero T, Couronné L, Khiabanian H, et al. Recurrent mutations in epigenetic regulators, RHOA and FYN kinase in peripheral T cell lymphomas. *Nat Genet*. 2014;46(2):166-170.
58. Sakata-Yanagimoto M, Enami T, Yoshida K, et al. Somatic RHOA mutation in angioimmunoblastic T cell lymphoma. *Nat Genet*. 2014;46(2):171-175.
59. Yoo HY, Sung MK, Lee SH, et al. A recurrent inactivating mutation in RHOA GTPase in angioimmunoblastic T cell lymphoma. *Nat Genet*. 2014;46(4):371-375.
60. Wilcox RA. A three-signal model of T-cell lymphoma pathogenesis. *Am J Hematol*. 2016;91(1):113-122.
61. Serwold T, Hochedlinger K, Swindle J, Hedgpeth J, Jaenisch R, Weissman IL. T-cell receptor-driven lymphomagenesis in mice derived from a reprogrammed T cell. *Proc Natl Acad Sci USA*. 2010;107(44):18939-18943.
62. Liang PI, Chang ST, Lin MY, et al. Angioimmunoblastic T-cell lymphoma in Taiwan shows a frequent gain of ITK gene. *Int J Clin Exp Pathol*. 2014;7(9):6097-6107.
63. Young RM, Shaffer AL III, Phelan JD, Staudt LM. B-cell receptor signaling in diffuse large B-cell lymphoma. *Semin Hematol*. 2015;52(2):77-85.
64. Piccaluga PP, Tabanelli V, Pileri SA. Molecular genetics of peripheral T-cell lymphomas. *Int J Hematol*. 2014;99(3):219-226.
65. Saveliev A, Vanes L, Ksionda O, et al. Function of the nucleotide exchange activity of vav1 in T cell development and activation. *Sci Signal*. 2009;2(101):ra83.
66. Lazer G, Pe'er L, Farago M, Machida K, Mayer BJ, Katzav S. Tyrosine residues at the carboxyl terminus of Vav1 play an important role in regulation of its biological activity. *J Biol Chem*. 2010;285(30):23075-23085.
67. Faruqi TR, Gomez D, Bustelo XR, Bar-Sagi D, Reich NC. Rac1 mediates STAT3 activation by autocrine IL-6. *Proc Natl Acad Sci USA*. 2001;98(16):9014-9019.
68. Chiarle R, Simmons WJ, Cai H, et al. Stat3 is required for ALK-mediated lymphomagenesis and provides a possible therapeutic target. *Nat Med*. 2005;11(6):623-629.
69. Jerez A, Clemente MJ, Makishima H, et al. STAT3 mutations unify the pathogenesis of chronic lymphoproliferative disorders of NK cells and T-cell large granular lymphocyte leukemia. *Blood*. 2012;120(15):3048-3057.
70. Chen YW, Guo T, Shen L, et al. Receptor-type tyrosine-protein phosphatase κ directly targets STAT3 activation for tumor suppression in nasal NK/T-cell lymphoma. *Blood*. 2015;125(10):1589-1600.
71. van der Fits L, Out-Luiting JJ, Tensen CP, Zoutman WH, Vermeer MH. Exploring the IL-21-STAT3 axis as therapeutic target for Sézary syndrome. *J Invest Dermatol*. 2014;134(10):2639-2647.
72. Lazaridis KN, McAllister TM, Babovic-Vuksanovic D, et al. Implementing individualized medicine into the medical practice. *Am J Med Genet C Semin Med Genet*. 2014;166C(1):15-23.
73. Iida S. Overview: A New Era of Cancer Genomics in Lymphoid Malignancies. *Oncology*. 2015;89(Suppl 1):4-6.
74. O'Connor OA, Bhagat G, Ganapathi K, et al. Changing the paradigms of treatment in peripheral T-cell lymphoma: from biology to clinical practice. *Clin Cancer Res*. 2014;20(20):5240-5254.
75. Zeng Y, Feldman AL. Genetics of anaplastic large cell lymphoma. *Leuk Lymphoma*. 2015;57(1):1-7.
76. Swerdlow SH, Campo E, Harris NL, et al, eds. WHO Classification of Tumours of Haematopoietic and Lymphoid Tissues. WHO/IARC Classification of Tumours, 4th ed. Vol 2. Lyon, France: International Agency for Research on Cancer; 2008:269-320.
77. Roskoski R Jr. The ErbB/HER family of protein-tyrosine kinases and cancer. *Pharmacol Res*. 2014;79:34-74.
78. Gupta M, Stenson M, O'Byrne M, et al. Comprehensive serum cytokine analysis identifies IL-1RA and soluble IL-2R α as predictors of event-free survival in T-cell lymphoma. *Ann Oncol*. 2016;27(1):165-172.

79. Zimmermann M, et al. Mutations Targeting the ErbB Pathway and MSC in Peripheral T-Cell Lymphoma. *Blood*. 2015;126:2681.
80. Challa-Malladi M, Lieu YK, Califano O, et al. Combined genetic inactivation of β 2-Microglobulin and CD58 reveals frequent escape from immune recognition in diffuse large B cell lymphoma. *Cancer Cell*. 2011;20(6):728-740.
81. Yoshida N, Karube K, Utsunomiya A, et al. Molecular characterization of chronic-type adult T-cell leukemia/lymphoma. *Cancer Res*. 2014;74(21):6129-6138.
82. Ougolkov AV, Billadeau DD. Targeting GSK-3: a promising approach for cancer therapy? *Future Oncol*. 2006;2(1):91-100.
83. Choi E, Han C, Park I, et al. A novel germ cell-specific protein, SHIP1, forms a complex with chromatin remodeling activity during spermatogenesis. *J Biol Chem*. 2008;283(50):35283-35294.
84. Premack BA, Gardner P. Signal transduction by T-cell receptors: mobilization of Ca and regulation of Ca-dependent effector molecules. *Am J Physiol*. 1992;263(6 Pt 1):C1119-C1140.
85. Nuytten M, Beke L, Van Eynde A, et al. The transcriptional repressor NIPP1 is an essential player in EZH2-mediated gene silencing. *Oncogene*. 2008;27(10):1449-1460.
86. Shi M, Shahsafaei A, Liu C, Yu H, Dorfman DM. Enhancer of zeste homolog 2 is widely expressed in T-cell neoplasms, is associated with high proliferation rate and correlates with MYC and pSTAT3 expression in a subset of cases. *Leuk Lymphoma*. 2015;56(7):2087-2091.
87. Anderson MW, Zhao S, Freud AG, et al. CD137 is expressed in follicular dendritic cell tumors and in classical Hodgkin and T-cell lymphomas: diagnostic and therapeutic implications. *Am J Pathol*. 2012;181(3):795-803.
88. Rohr J, et al. Recurrent activating mutations of CD28 in peripheral T-cell lymphomas. *Leukemia*. 2016;30(5):1062-1070.
89. Meijerink JP, Mensink EJ, Wang K, et al. Hematopoietic malignancies demonstrate loss-of-function mutations of BAX. *Blood*. 1998;91(8):2991-2997.